Acta Biomed 2017; Vol. 88, N. 3: 319-324 DOI: 10.23750/abm.v%vi%i.5181

Case report

Enlarged Virchow-Robin spaces in a young man: a constrained spherical deconvolution tractography study

Alberto Cacciola[1,2], Rocco Salvatore Calabrò[1], Antonio Costa[1], Antonino Naro[1], Demetrio Milardi[1,2], Daniele Bruschetta[2]

[1]IRCCS Centro Neurolesi "Bonino Pulejo", Messina, Italy; [2] Department of Biomedical Sciences and Morphological and Functional Images, University of Messina, Italy

Summary. *Background and aim:* Virchow-Robin spaces are mainly located along the path of the lenticulostriate arteries in the basal ganglia through the anterior perforate substance, and can be found both in normal subjects, as a rare phenomenon, and in patients with different diseases. We report a case of a healthy young man with unilateral enlarged Virchow-Robin spaces in the left capsule-lenticulostriate area. Aim of this case report is to show the potential of probabilistic Constrained Spherical Deconvolution (CSD) tractography in showing abnormal diffusion tensor imaging and tractography of the anterior thalamic tracts caused by mass effect from adjacent enlarged Virchow-Robin spaces. *Methods:* The study was performed with a 3T magnetic resonance imaging (MRI) scanner (Achieva, Philips Healthcare, Best, Netherlands); equipped with a 32-channel SENSE head coil. Diffusion Weighted Images were analyzed by using CSD, a fast computation method that overcomes major limitations of Diffusion Tensor Imaging allowing reliable estimation of one or more fiber orientations in the presence of intravoxel orientational heterogeneity. *Results:* Tractography showed increased Fractional Anisotropy and reduced Apparent Diffusion Coefficient values, a displacement and compression of the anterior thalamic projections by part of the enlarged VRS, and a decrease of white matter fibers in the left side in comparison to the right one. *Conclusions:* We report on a case of a healthy individual with unilateral dilated VRS in the capsulo-lenticulostriatal area, proving the utility of diffusion MRI and tractography in understanding the abnormal neuroanatomy of this particular condition. (www.actabiomedica.it)

Key words: CSD, tractography, Virchow-Robin spaces, DTI; fibres

Introduction

In 1859, Robin was the first to describe the perivascular spaces as canals surrounding the walls of the blood vessels along their course in the subarachnoid space through the brain parenchyma (1).

Enlarged Virchow-Robin spaces (VRS) can be seen on MRI as round or cystic lesions, isointense to cerebrospinal fluid (CSF). Diffusion Tensor Imaging (DTI) and fiber tractography may allow evaluating and detecting white matter fiber bundle alterations in several cerebral structural abnormalities. Constrained spherical deconvolution (CSD) is a fast computation method that overcomes the major limitations of DTI, allowing to reliably estimate fiber orientation in presence of intravoxel heterogeneity (2-4). Herein, we report a case of a healthy individual with unilaterally dilated VRS in the capsule- lenticulo-striatal area, proving for the first time the utility of CSD-based tractography in understanding the abnormal neuroanatomy of this particular condition.

Case report

An otherwise healthy 24 year-old male underwent a brain MRI as volunteer for a neuroimaging protocol approved by our Ethical Committee. Written informed consent was signed from the subject before MRI examination. Since the basal MRI showed an abnormal dilatation of the VRS in the left capsule-lenticulo- striatal area, we decided to investigate whether such abnormalities somehow led to fiber bundle alterations. The study was performed with a 3-T Achieva Philips scanner using a 32-channel SENSE head coil. Three-dimensional (3D) high-resolution T1-weighted fast field echo (FFE), 3D high resolution T2 weighted Turbo Spin Echo (TSE), and dual phase-encoded pulsed- gradient spin-echo diffusion weighted sequences (DWI) were obtained. DWIs were acquired at a b-value of 1000 s/mm2, using 60-gradient diffusion directions chosen following the rules stated by an electrostatic repulsion model. We created a brain mask image in order to remove noisy voxels outside the brain, and to avoid tracks generated by the fiber-tracking algorithm from propagating outside the head. For this reason, the brain mask should have the same dimensions as the DWI data set and the easiest way is to extract the b=0 image from the DWI data set. The next step was to generate various tensor maps, such as Fractional Anisotropy (FA) and Apparent Diffusion Coefficient (ADC). Then, we reconstructed a colour-coded map in which red, blue, and green colours indicated the principal eigenvector's directions (5). Specifically, the red colour indicated a left-to-right pattern, the green colour an anterior-to-posterior, and the blue colour a caudal-to- cranial one. We used a modified High Angular Resolution Diffusion Imaging (HARDI) technique, called non-negativity CSD, which estimates the fiber Orientation Distribution Function (fODF) directly from the DW signals by means of positive spherical deconvolution (avoiding the unreal negative regions) (2). In order to obtain robust measurements despite the presence of noise, we set the maximal spherical harmonic degree to eight. Concerning the identification of fiber orientations, the fODF was calculated deconvolving the spherical fitted model obtained by a single-fiber estimated response. Regions-of-interest (ROIs) were drawn on axial slices in the anterior limb of the internal capsule and in the thalamus. Fiber-tracking was performed using the MRtrix package (Tournier JD, Brain Research Institute, Melbourne, Australia, http://www.brain.org.au/software/). The step size of the streamlines tracking algorithm was set at 0.2 mm, the minimum radius of curvature at 1 mm, and the FA/FOD amplitude cut-off for terminating tracks was 0.1. Tractography showed increased FA and reduced ADC values, a displacement and compression of the anterior thalamic (AT) projections by part of the enlarged VRS, and a decrease of white matter fibers in the left side in comparison to the right one (Fig. 1). Quantitative analysis in the right side revealed a FA value of 0.397755, an ADC value of 0.630322×10–3 mm2/s, and a number (N) of streamlines=1000, whilst the left AT presented a FA=0.418604 ($p=0.01$), an ADC=0.576638×10–3 mm^2/s ($p=0.002$), and a N=565 ($p<0.001$).

Discussion

VRS enlargements can be located along: i) the path of the lenticulo-striate arteries in the basal ganglia through the anterior perforate substance; ii) the course of the medullar perforating arteries when they enter the cortical gray matter over the convexity and extend into the white matter; and iii) the ponto-mesencephalic junction, although rarely (6). They can be found either in normal subjects, as a rare phenomenon, or in patients with different diseases. Indeed, their proved function as pathways for protein diffusion among different cellular compartments and for interstitial fluid drainage, could explain how enlarged VRS may be involved in several diseases, including inflammatory, vascular or metabolic conditions (7).

The differential diagnosis of VRS should include multiple sclerosis, acute and chronic lacunar infarct and cystic brain tumors. For example, acute lacunar infarcts can be detected as hypointense wedge-shaped regions on ADC map, whilst enlarged VRSs have a circular or linear purely cystic structure (8).

To the best of our knowledge, although cases of VRS widening have been extensively reported in literature, only few case reports explored DTI changes and tractography abnormalities in middle-aged patients (Table 1) (8-11).

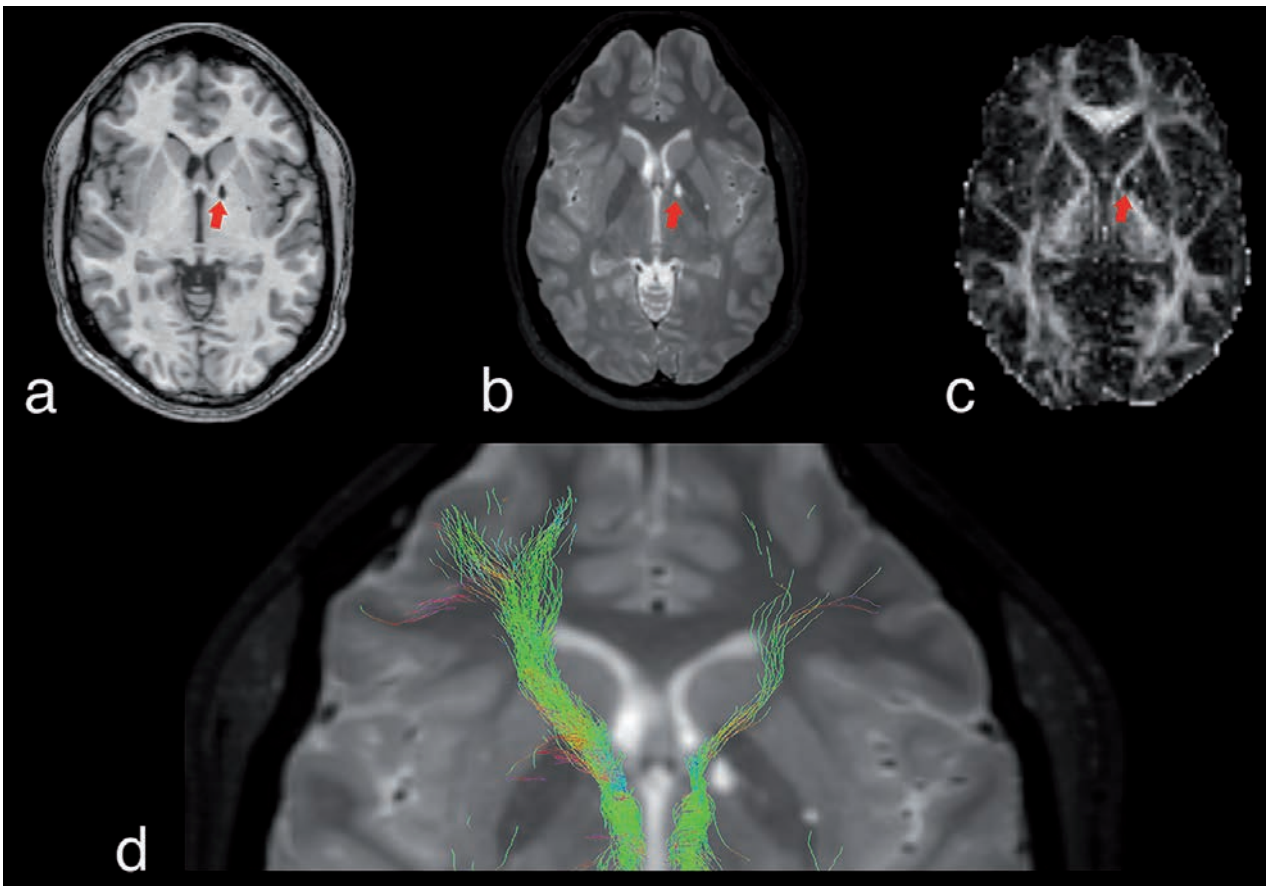

Figure 1. Morphologic MR imaging. (a) Axial 3D high-resolution T1-weighted Fast Field Echo image, (b) 3D high-resolution T2-weighted Turbo Spin Echo, and (c) fractional anisotropy map show dilated Virchow-Robin spaces (red arrows), isointense to cerebrospinal fluid, in capsule region. (d) The tractography shows a decrease of the white matter tracts in the left side as compared to the right one

Indeed, for the first time ever, we showed that CSD-based tractography is able to detect in vivo fiber bundle anomalies derived from enlarged VRS in a healthy man.

Indeed, tractography showed an asymmetry of white matter tracts in the ROIs of the left side in comparison to the right one, including a decrease of the number of streamlines, a distorted and compressed trajectory of AT projections through the anterior limb of internal capsule (Fig. 2, 3), and modifications of the anisotropy fraction and ADC. Noteworthy, FA describes to what extent water diffusion occurs anisotropically, and it is thought to be related to white matter integrity, since FA reduction may indicate white matter damage. In this patient, the increase of FA within the tracts surrounding dilated VRS may be due to subtle mass effect on the AT projections, finally leading to less extracellular fluid accumulation, and suggesting augmented diffusion anisotropy and structural coherence. On the other hand, ADC reflects the total magnitude of diffusion and therefore provides information about alterations in the extracellular volume of both grey and white matter (12, 13). To this regard, we reported reduced ADC values in the left side, thus suggesting a diminished diffusion magnitude and confirming previous in vitro findings showing that decreased extracellular spaces cause a decrease of ADC (14). In our healthy young man, the VRS dilations within the white matter of the left anterior limb of internal capsule were fortuitously discovered since he did not present any neurological symptoms or signs. Thus, diffusion tensor alterations do not necessarily predict any pathological condition.

The main limitations of the present study are related to the intrinsic weakness of the tractography

Table 1. Summary of enlarged VRS cases explored by DTI and tractography

Author	Year	Country	Type of study	Technique	Location	Symptoms	Findings
Algin et al. (8)	2012	Turkey Italy	Case Report Literature Review	DTI	Patient 1 and 2: left midbrain Patient 3: right midbrain and thalamus	Patient 1: dysphoric symptoms Patient 2: deficit at the right upper and lower limbs; diplopia Patient 3: loss of vision	Fibers were displaced through the periphery of enlarged VRS
Young et al. (9)	2014	USA	Case Report	DTI	Thalamus and ventral midbrain	No signs or symptoms of motor weakness	Increased FA, decreased MD, and compression at tractography
Ranjan et al. (10)	2013	Canada	Case Report	DTI	Dorsal pons	Trigeminal neuralgia	Distortion of the intrinsic trigeminal pathway
Mathias et al. (11)	2007	France	Case Report	DTI	Patient 1: frontal, precentral gyri and corpus callosum Patient 2: left superior and inferior parietal lobules and left middle and inferior temporal gyri	No clinical neurologic and neuropsychological signs or symptoms	Patients 1 and 2: decrease of white matter fibers in the pathologic areas compared with the healthy side

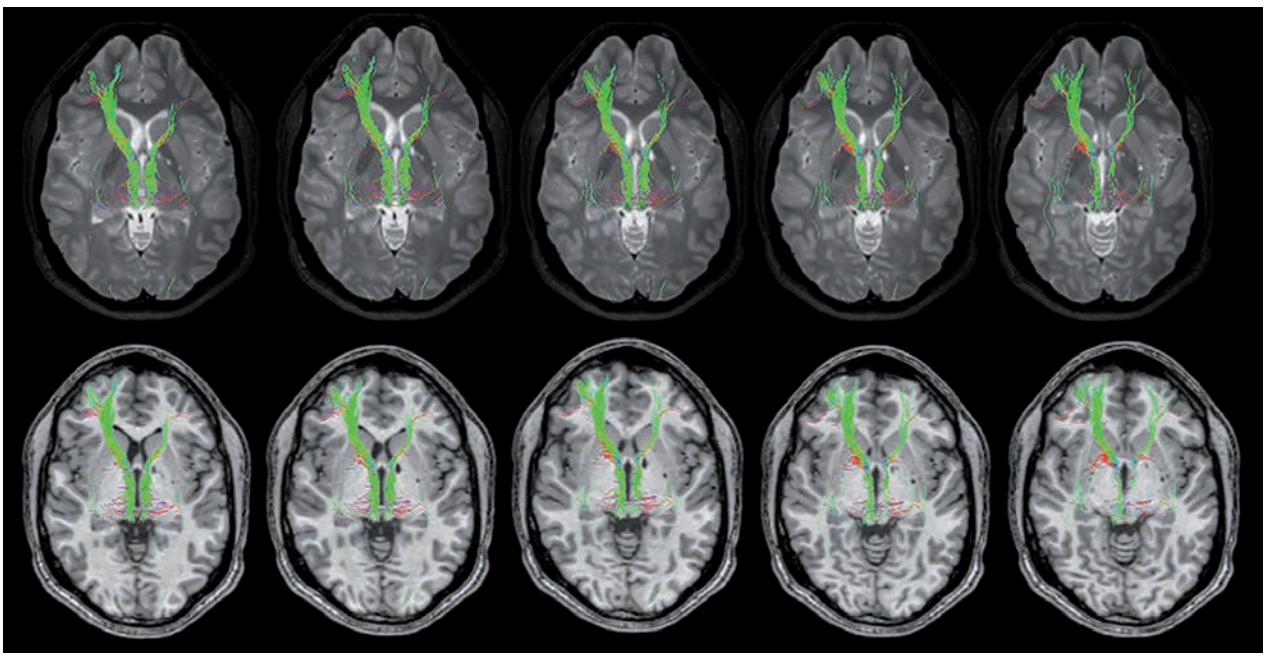

Figure 2. Axial 3D high-resolution T1-weighted Fast Field Echo and (first row) and 3D high-resolution T2-weighted Turbo Spin Echo (second row) sequences highlight the reduction and the abnormalities of the course of the anterior thalamic projections, which were decreased and compressed in the left side

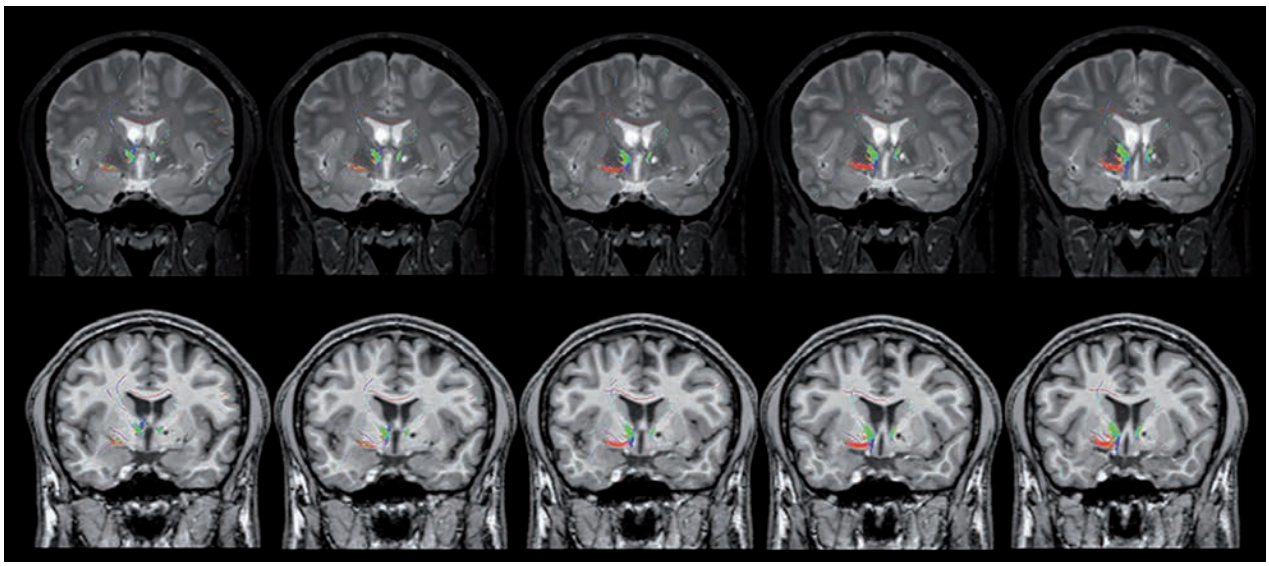

Figure 3. Coronal 3D high-resolution T1-weighted Fast Field Echo and (first row) and 3D high-resolution T2-weighted Turbo Spin Echo (second row) sequences highlight the reduction and the abnormalities of the course of the anterior thalamic projections, which were decreased and compressed in the left side

technique, which is a method based on the preferential anisotropic diffusion along the myelinated white matter. However, although tractography should be considered only as the highest mathematical probability of the existence of a given anatomical pathway, it has been previously shown that CSD is a valuable technique allowing a reliable reconstruction of long and short fiber pathways, also in those brain regions with complex fiber configurations (crossing, fanning, merging, bending, and kissing). Moreover, CSD overcomes partial volume effects associated with DTI, longer acquisition time of Diffusion Spectrum Imaging (15), and improves the poor angular resolution achieved with Q-balls Imaging.

In conclusion, DWI and CSD could be useful in the management of these lesions and allowed us to accurately detect abnormal diffusion tensor values and aberrant fiber trajectory secondary to unilateral dilation of VRS, which may be considered an incidental finding of uncertain clinical significance.

Acknowledgment

We would like to thank Prof. Placido Bramanti, Science Manager of I.R.C.C.S. "Centro Neurolesi", Messina, Italy, for the helpful collaboration.

References

1. Song CJ, Kim JH, Kier EL, Bronen RA. MR imaging and histologic features of subin- sular bright spots on T2-weighted MR images: Virchow-Robin spaces of the extreme capsule and insular cortex. Radiology 2000; 214: 671-77.
2. Tournier JD, Calamante F, Connelly A. Robust determination of the fibre orientation distribution in diffusion MRI: non-negativity constrained super-resolved spherical deconvolution. Neuroimage 2007; 35: 1459-1472.
3. Cacciola A, Milardi D, Calamuneri A, et al. Constrained spherical deconvolution tractography reveals cerebello - mammillary connections in humans. Cerebellum 2017; 16: 483-495.
4. Milardi D, Cacciola A, Cutroneo G, et al. Red nucleus connectivity as revealed by constrained spherical deconvolution tractography. Neurosci Lett 2016; 626: 68-73.
5. Pajevic S, Pierpaoli C. Colour schemes to represent the orientation of anisotropic tissues from diffusion tensor data: application to white matter fiber tract mapping in the human brain. Magn Reson Med 1999; 42: 526-540.
6. Ogawa T, Okudera T, Fukasawa H, et al. Unusual widening of Virchow-Robin spaces: MR appearance. AJNR Am J Neuroradiol 1995; 16: 1238-42.
7. Zhu YC, Dufouil C, Mazoyer B, et al. Frequency and location of dilated Virchow-Robin spaces in elderly people: a population-based 3D MR imaging study. AJNR Am J Neuroradiol 2011; 32: 709-13.
8. Algin O, Conforti R, Saturnino PP, et al. Giant dilatations of virchow-robin spaces in the midbrain. MRI aspects and review of the literature. Neuroradiol J 2012; 25: 415-22.
9. Young RJ, Lee V, Peck KK, et al. Diffusion tensor imaging

and tractography of the corticospinal tract in the presence of enlarged Virchow-Robin spaces. J Neuroimaging 2014; 24: 79-82.
10. Ranjan M, Dupre S, Honey CR. Trigeminal neuralgia secondary to giant Virchow-Robin spaces: a case report with neuroimaging. Pain 2013; 154: 617-9.
11. Mathias J, Koessler L, Brissart H, et al. Giant cystic widening of Virchow-Robin spaces: an anatomofunctional study. AJNR Am J Neuroradiol 2007; 28: 1523-5.
12. Basser PJ, Pierpaoli C. Microstructural and physiological features of tissues elucidated by quantitative-diffusion-tensor MRI. Magn Reson B 1996; 111: 209-19.
13. Le Bihan D. Looking into the functional architecture of the brain with diffusion MRI. Nat Rev Neurosci 2003; 4: 469-80.
14. Anderson AW, Zhong J, Petroff OA, et al. Effects of osmotically driven cell volume changes on diffusion-weighted imaging of the rat optic nerve. Magn Reson Med 1996; 35: 162-167.
15. Tournier JD, Yeh CH, Calamante F, Cho KH, Connelly A, Lin CP. Resolving crossing fibres using constrained spherical deconvolution: validation using diffusion-weighted imaging phantom data. Neuroimage 2008; 42: 617-625.

Received: 1 February 2016
Accepetd: 2 May 2016
Correspondance:
Alberto Cacciola
Department of Biomedical Sciences and Morphological and Functional Images, University of Messina,
98125 Messina, Italy
Tel. +39 0902217143
E-mail: alberto.cacciola0@gmail.com